Thermochimica Acta, 181 (1991) 127–141
Elsevier Science Publishers B.V., Amsterdam

SIMULTANEOUS MEASUREMENT OF EXCESS ENTHALPIES AND SOLUTION DENSITIES IN A FLOW CALORIMETER

W.K. TOLLEY * and R.M. IZATT **

Department of Chemistry, Brigham Young University, Provo, UT 84602 (U.S.A.)

J.L. OSCARSON

Department of Chemical Engineering, Brigham Young University, Provo, UT 84602 (U.S.A.)

(Received 4 September 1990)

ABSTRACT

The addition of a densitometer to the flow calorimeters developed earlier made possible the simultaneous measurement of heats of mixing (H_m^E) and solution densities. The availability of H_m^E and density data measured at the same temperature–pressure coordinates should be useful in developing more accurate models of fluid behavior in the critical region. The instrument was used to measure H_m^E and density values for the systems *n*-hexane + CO_2 and neopentane + CO_2.

INTRODUCTION

Understanding and predicting the rapid changes in fluid properties which occur in the critical region present a challenge in theoretical chemistry. The understanding of critical behavior has application both to pure compounds and to fluid mixtures. A thorough understanding of the chemistry in the critical region will facilitate application of this novel chemistry to innovative separations, such as supercritical fluid chromatography [1], separating azeotropic mixtures [2], or fractionating low vapor-pressure compounds [3].

The recent development of precision flow calorimeters has made possible the collection of heat of mixing (H_m^E) data on near-critical fluids [4,5]. These H_m^E data have been used to explain solubilities in supercritical fluids [6]. In addition, solution volume has been related to solubility near the critical point [6]. Wells et al. [7] showed that density-based correlations predict solubility in supercritical fluids better than traditional equations of state, but noted the difficulty in obtaining experimentally measured densities of these

* Taken in part from Ph.D. dissertation, Brigham Young University, December 1990.
** Author for correspondence.

0040-6031/91/$03.50

fluids. A complete description of critical phenomena requires knowledge of the energy, derived from excess enthalpy measurements, and PVT behavior, which can be derived from density measurements.

In this paper, we describe a flow calorimeter to which has been added a densitometer enabling the simultaneous measurement of H_m^E and fluid density values. Both the calorimeter and the densitometer are linked to a computer, which collects, analyzes, and stores data from both instruments.

EXPERIMENTAL

Equipment

The calorimeter, depicted in Fig. 1, is a modification of the isothermal flow calorimeter described by Christensen et al. [5]. Stainless steel tubing, a calibration heater, and a control heater were wrapped securely around a copper cylinder of 1.25 cm outside diameter. A Peltier (thermoelectric) cooler was clamped to the top of the cylinder. A thermistor was secured inside a hole drilled near the top of the cylinder to monitor temperature. As with the earlier calorimeter [5], the Peltier device continuously removed heat from the copper cylinder. The control heater continuously added heat to counteract the cooling effect and maintain isothermal conditions of the

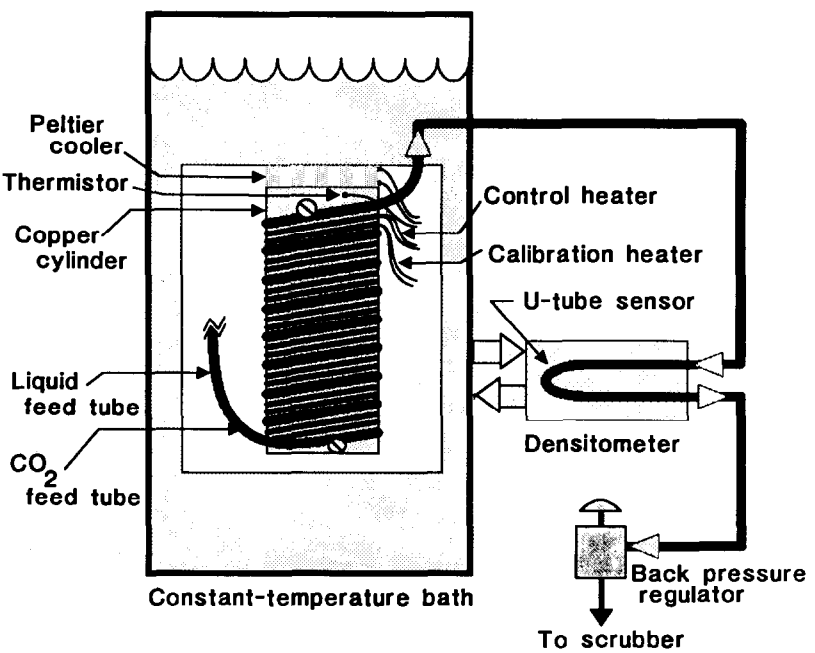

Fig. 1. Schematic of high-pressure flow calorimeter.

cylinder. Other sources of temperature change, such as the heat change during fluid mixing, are detected as changes in the power consumption of the control heater.

Reagents were fed into the calorimeter by ISCO LC-5000 syringe pumps which were connected to the liquid and CO_2 feed tubes. The pump controllers interfaced with the computer which operated the calorimeter. Pump flows could be set independently under computer control for rates between 1 and 400,000 $\mu l\ h^{-1}$ at pressures to 41 MPa. Check valves on the pump outlets impeded inadvertent reverse flow into the pumps. Teflon seals were put into the check valves to avoid degradation resulting from contact with the reagents.

The electronic controllers for the calorimeter were built by Tronac, Inc. A Tronac model 550 isothermal adaptor powered the control heater on the isothermal cylinder and monitored power consumption. A Tronac model 450 calorimeter controller powered the calibration heater. A Tronac model 900 computer interface converted the BCD-format data from the densitometer into ASCII code and transferred the heat and density readings to the computer.

The fluid leaving the calorimeter flowed through a Paar DMA 512 ultrasonic densitometer. Oil from the constant temperature bath passed through a heat exchanger in the densitometer to maintain the temperature of the fluid during density measurements. Oil flowed by suction through the heat exchanger and was pumped back to the constant temperature bath so that viscous heating of the oil from pumping occurred after the oil had passed through the densitometer. The precision of the density readings was 0.001 $g\ cm^{-3}$.

Calibration of the densitometer was accomplished using CO_2 and hexane. Density data for CO_2 were taken from IUPAC data [8]. Hexane density was reported by Diaz Pena and Tardajos [9].

Pressure within the calorimeter was monitored with a Bourdon-tube gauge attached to the CO_2 feed line. The gauge was calibrated with a dead-weight tester before use. Pressure transducers in each pump provided electronic pressure readings that could be accessed by the computer. Pressure was controlled by a Grove back-pressure regulator downstream from the calorimeter and densitometer. Pressure hysteresis was usually less than 0.05 MPa.

Materials

Coleman Instrument-grade CO_2 from local suppliers was used without further treatment. It was fed directly into the pump under tank pressure. Hexane (Phillips Petroleum) was obtained in Phillips Pure grade (99 mol.% minimum purity). This reagent was filtered, dehydrated using metallic sodium, and degassed ultrasonically before use. Neopentane (2,2-dimethyl-

TABLE 1

Excess enthalpies of mixing (H_m^E) values for *n*-hexane + CO_2 and densities (ρ) of resultant solutions at the specified temperatures and pressures

x (Hexane)	H_m^E (J mol^{-1})	ρ (kg dm^{-3})	x (Hexane)	H_m^E (J mol^{-1})	ρ (kg dm^{-3})
7.50 MPa	308.15 K				
0.000	0	0.358	0.503	−1681	0.699
0.024	−2468	0.584	0.544	−1459	0.694
0.065	−4060	0.716	0.583	−1320	0.690
0.103	−3983	0.724	0.623	−1136	0.685
0.143	−3690	0.731	0.663	−969	0.681
0.184	−3450	0.732	0.703	−791	0.677
0.224	−3318	0.730	0.743	−612	0.672
0.264	−3062	0.727	0.783	−440	0.669
0.303	−2815	0.722	0.822	−328	0.666
0.343	−2592	0.718	0.863	−237	0.664
0.383	−2269	0.713	0.903	−107	0.660
0.423	−2144	0.708	0.942	−42	0.658
0.463	−1842	0.704	1.000	0	0.654
10.5 MPa	308.15 K				
0.000	0	0.739	0.512	655	0.705
0.021	0	0.748	0.552	651	0.701
0.062	43	0.758	0.592	627	0.696
0.104	126	0.760	0.631	620	0.692
0.145	214	0.757	0.671	598	0.686
0.187	304	0.752	0.710	551	0.684
0.228	385	0.747	0.749	458	0.678
0.269	460	0.740	0.788	403	0.674
0.310	522	0.734	0.827	329	0.671
0.351	571	0.728	0.865	251	0.667
0.391	610	0.722	0.904	171	0.664
0.432	631	0.716	0.943	61	0.661
0.472	648	0.711	1.000	0	0.658
12.5 MPa	308.15 K				
0.000	0	0.783	0.505	829	0.710
0.021	59	0.784	0.545	810	0.705
0.062	192	0.783	0.585	777	0.699
0.103	331	0.777	0.625	747	0.695
0.144	446	0.770	0.665	697	0.690
0.184	537	0.763	0.704	637	0.686
0.225	622	0.757	0.744	567	0.681
0.265	689	0.748	0.784	500	0.677
0.305	738	0.741	0.823	415	0.674
0.345	780	0.735	0.862	307	0.670
0.385	817	0.727	0.902	210	0.667
0.425	830	0.722	0.941	107	0.664
0.465	836	0.716	1.000	0	0.660

TABLE 1 (continued)

x (Hexane)	H_m^E (J mol^{-1})	ρ (kg dm^{-3})	x (Hexane)	H_m^E (J mol^{-1})	ρ (kg dm^{-3})
6.29 MPa	313.15 K				
0.000	0	0.166	0.540	−2273	0.689
0.020	−226	★	0.580	−2063	0.684
0.060	−986	★	0.620	−1639	0.681
0.100	−1535	★	0.660	−1559	0.679
0.140	−2252	★	0.700	−1422	0.675
0.180	−2724	★	0.740	−1094	0.672
0.220	−3299	★	0.780	−935	0.671
0.260	−3954	0.712	0.820	−708	0.668
0.300	−3943	0.712	0.860	−538	0.662
0.340	−3627	0.710	0.900	−381	0.664
0.380	−3454	0.708	0.940	−266	0.663
0.420	−3013	0.701	0.980	−140	0.661
0.460	−2718	0.697	1.000	0	0.649
0.500	−2477	0.695			
7.5 MPa	313.15 K				
0.000	0	0.262	0.536	−1691	0.687
0.059	−2506	0.635	0.576	−1495	0.684
0.099	−3999	0.690	0.616	−1308	0.679
0.138	−3877	0.709	0.657	−1118	0.676
0.178	−3696	0.714	0.697	−939	0.675
7.5 MPa	313.15 K				
0.217	−3479	0.715	0.737	−786	0.670
0.257	−3257	0.714	0.778	−650	0.668
0.297	−3018	0.711	0.817	−520	0.668
0.337	−2784	0.707	0.858	−399	0.666
0.376	−2505	0.705	0.898	−236	0.661
0.416	−2324	0.701	0.939	−179	0.658
0.456	−2099	0.697	1.000	0	0.651
0.496	−1890	0.693			
8.36 MPa	313.15 K				
0.000	0	0.486	0.418	−1482	0.703
0.020	−726	0.516	0.459	−1303	0.699
0.060	−2720	0.651	0.498	−1187	0.694
0.099	−2861	0.688	0.538	−1077	0.688
0.139	−2786	0.705	0.578	−906	0.686
0.179	−2667	0.717	0.618	−720	0.674
0.219	−2457	0.720	0.658	−639	0.671
0.259	−2231	0.719	0.699	−449	0.672
0.299	−2026	0.715	0.739	−375	0.672
0.339	−1830	0.709	1.000	0	0.653
0.378	−1656	0.698			

TABLE 1 (continued)

x (Hexane)	H_m^E (J mol^{-1})	ρ (kg dm^{-3})	x (Hexane)	H_m^E (J mol^{-1})	ρ (kg dm^{-3})
10.5 MPa	313.15 K				
0.000	0	0.679	0.540	259	0.692
0.060	−259	0.732	0.580	360	0.690
0.100	−257	0.730	0.620	363	0.683
0.140	−207	0.733	0.660	351	0.681
0.180	−134	0.736	0.700	334	0.679
0.220	−63	0.733	0.740	312	0.674
0.260	14	0.730	0.780	271	0.668
0.300	79	0.724	0.820	199	0.665
0.340	140	0.717	0.860	138	0.663
0.380	196	0.715	0.900	92	0.661
0.420	232	0.708	0.940	79	0.661
0.460	299	0.706	1.000	0	0.655
0.500	331	0.700			
12.5 MPa	313.15 K				
0.000	0	0.742	0.540	631	0.697
0.060	77	0.754	0.580	626	0.694
0.100	144	0.757	0.620	569	0.688
0.140	227	0.748	0.660	566	0.685
0.180	308	0.748	0.700	524	0.683
0.220	309	0.743	0.740	465	0.677
0.260	447	0.739	0.780	415	0.673
0.300	523	0.732	0.820	348	0.671
0.340	578	0.729	0.860	272	0.668
0.380	621	0.721	0.900	194	0.664
0.420	627	0.715	0.940	111	0.662
0.460	647	0.711	1.000	0	0.657
0.500	639	0.705			

★ Two-phase region.

propane) was obtained from Matheson Gas Products, Inc., in minimum 99 mol.% purity, and was fed directly from a compressed-gas cylinder into the pump without further purification.

Procedures

The pumps were cooled to 17 °C when pumping CO_2 and neopentane to ensure that the fluids liquefied, thereby reducing variability in molar volumes. Hexane was pumped at ambient temperature. Typically, 30–60 min were allowed for the fluids in the pump to stabilize at the desired temperature and pressure during the initial pressurization.

Pump control and data collection were accomplished by computer control using an operating schedule selected by the operator. Total flow rates of

reagents during heat measurements typically ranged between 0.2 and 0.4 ml min^{-1} through the calorimeter. These flow rates were sufficiently low that viscous heating of the fluid was not observed. Higher flow rates were used occasionally when very small heats were anticipated. The sum of the molar flow rates from both pumps held constant throughout each test, which required that volumetric flow rates vary somewhat during each run.

For heat and density determinations, known proportions of each fluid were pumped into the calorimeter on command from the computer. The computer sampled the power consumption of the calorimeter and the density reading every 10 s until both had stabilized. Readings were monitored for at least 20 min to ensure stability, and usually stabilized within 40 min. The computer then averaged the power and densitometer readings over a 5 min period. The computer stored the averages, then instructed the pumps to change flow rates according to a program selected by the operator. Readings were commonly taken at mole-fraction intervals of 0.04.

Isothermal compressibilities were calculated for single-phase mixtures when a sufficient amount of density data was available. A least-squares regression was used to obtain a linear correlation between pressure and solution density at constant composition.

Excess volumes were calculated from the density data. At constant temperature and pressure, the excess volume of a mixture is

$$V^E = [(x_1 MW_2 + x_1 MW_2)/\rho_m] - [x_1 MW_1/\rho_1] - [x_2 MW_2/\rho_2] \quad (1)$$

where MW = formula weight of the component, ρ_m = density of the fluid mixture, and ρ_1, ρ_2 = densities of the pure components at the test conditions.

RESULTS AND DISCUSSION

Hexane + CO_2

The density and H_m^E data are presented in Table 1. The H_m^E data for tests at 308.15 K are plotted in Fig. 2a. The H_m^E data have been measured and reported earlier [10]. Although methods to extract phase data from excess enthalpy curves are described in the earlier publication, little interpretation of the data was presented. The linear portion of the heat curve for mixtures at 7.5 MPa (Fig. 2a) is attributed to the existence of a two-phase region. The H_m^E data indicate fluid–fluid immiscibility from $x < 0.01$ to $x = 0.03$ mole-fraction hexane. The spacing of the data points does not allow closer resolution of the phase boundaries. At higher pressures, the solutions remain as a single fluid phase at all compositions. This interpretation agrees with phase data for mixtures of normal alkanes and CO_2 [11].

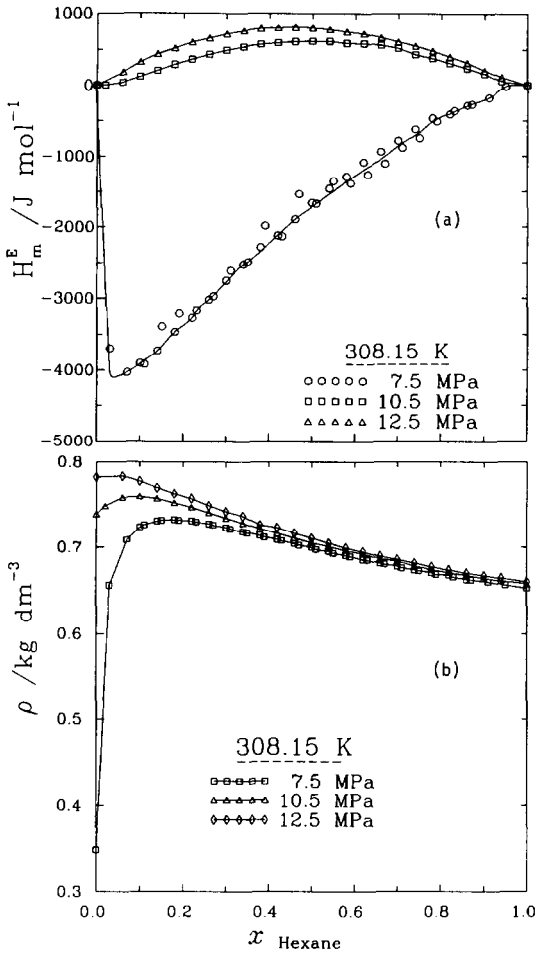

Fig. 2. a, H_m^E (hexane + CO_2) values as a function of composition at 308.15 K; b, densities of (hexane + CO_2) fluid mixtures as a function of composition at 308.15 K.

The absence of strong chemical interaction between CO_2 and hexane requires an alternative explanation for the large H_m^E values at 7.5 MPa. The negative H_m^E values arise because of the proximity of the interaction temperature/pressure of the fluids to the CO_2 critical point. A mathematical interpretation in terms of heat capacity of near-critical fluids has been discussed by Christensen et al. [12]. A qualitative explanation for the exothermic mixing derives from a consideration of the fluids. Liquid hexane at this temperature and pressure is much denser than the supercritical CO_2 and, as a result, has lower internal energy. Adding a small amount of hexane to the supercritical CO_2 causes the CO_2 to liquefy and release this stored energy. The maximum amount of heat that can be released per unit of mixture occurs at the saturated liquid boundary.

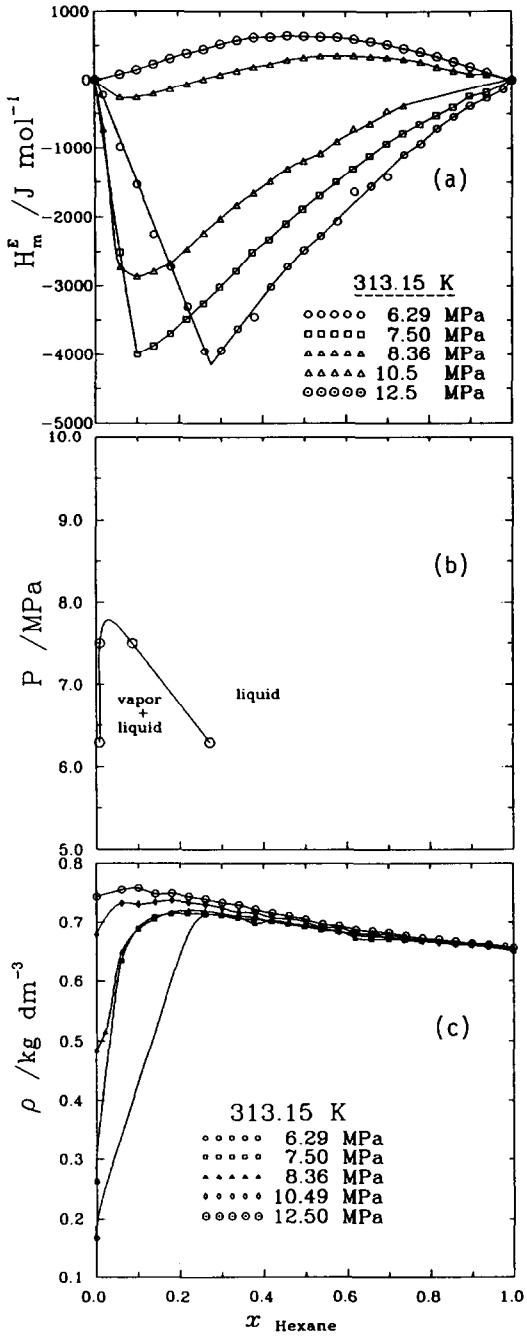

Fig. 3. a, H_m^E (hexane + CO_2) values as a function of composition at 313.15 K; b, pressure–composition diagram of (hexane + CO_2) at 313.15 K; c, densities of (hexane + CO_2) fluid mixtures as a function of composition at 313.15 K.

Supercritical CO_2 at 10.5 and 12.5 MPa is much more compressed than at 7.5 MPa. As a result, heats of mixing are endothermic except for a small region in the CO_2-rich solutions at 10.5 MPa.

Density data for solutions at 308.15 K are plotted in Fig. 2b. Densities at 7.5 MPa are seen to rise sharply as the hexane content of the fluids increases from 0 to 0.18 mole fraction. This is in accord with the interpretation of the fluid changing from a supercritical vapor to a liquid over this composition range. The density drops non-linearly through the hexane-rich region. Densities of solutions at 10.5 and 12.5 MPa follow a smooth change from the density of the highly compressed supercritical CO_2 component to that of the less dense liquid hexane.

The excess enthalpy data for 313.15 K are plotted in Fig. 3a. Heats at 7.5 MPa were similar at both 313.15 and 308.15 K. The minimum in the heat curve shifted slightly in the direction of higher hexane concentration with the increased temperature. The heat curves at 6.29 and 7.50 MPa appear to have fluid–fluid immiscibility in CO_2-rich solutions. The two-phase region

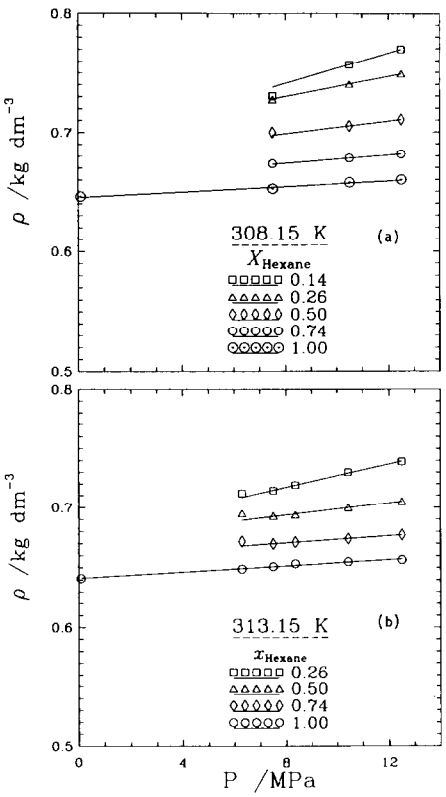

Fig. 4. a, Pressure–density plots of (hexane + CO_2) fluid mixtures at 308.15 K; b, pressure–density plots of (hexane + CO_2) fluid mixtures at 313.15 K.

TABLE 2

Isothermal compressibilities of hexane + CO_2 solutions

x (Hexane)	Compressibility (TPa^{-1})	
	308.15 K	313.15 K
0.140	11,200	–
0.260	5,890	7,050
0.500	2,900	3,500
0.740	2,340	2,230
1.000	1,690	1,850

disappeared at 8.36 MPa and above. The pressure–composition plot taken from the enthalpy data, Fig. 3b, agrees with data reported by Schneider [11].

At higher pressures (10.5 and 12.5 MPa), the CO_2 at 313.15 K is measurably more gas-like than at 308.15 K. As a result, the interactions are more exothermic.

Densities of the (hexane + CO_2) solutions at 313.15 K are plotted in Fig. 3c. Density readings were somewhat erratic through the two-phase region at 6.29 MPa because of the inhomogeneous fluid and the large difference in density between the vapor and the liquid. These density readings were not included in the plot.

The density data provide the information needed to calculate isothermal compressibilities for the solutions. As shown in Fig. 4a and b, the solution densities varied linearly with pressure within experimental error. Isothermal compressibility values calculated from the slopes of these plots are recorded

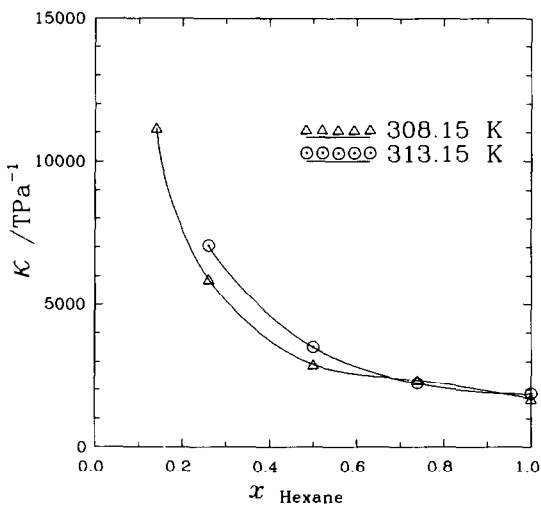

Fig. 5. Isothermal compressibilities of (hexane + CO_2) fluid mixtures as a function of composition.

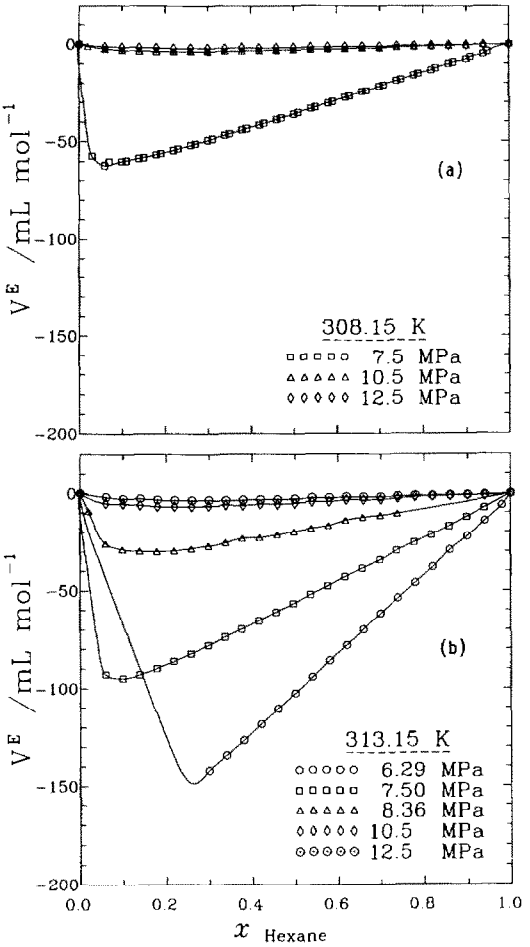

Fig. 6. a, V^E (hexane + CO_2) values as a function of composition at 308.15 K; b, (hexane + CO_2) values as a function of composition at 313.15 K.

in Table 2 and plotted in Fig. 5. The compressibilities of hexane-rich solutions is seen to be less than those of CO_2-rich solutions, in keeping with the higher compressibility of supercritical CO_2 in comparison with liquid hexane. The compressibilities of the solutions increased as the temperature increased. This increase can be explained by the tendency of fluids to be more gas-like at higher temperature. The compressibilities of pure hexane interpolated from the literature are 1831 and 1925 TPa^{-1} at 308.15 and 313.15 K, respectively [9]. These values are in good agreement with that given in Table 2.

The density data also allowed calculation of excess volumes, which are another measure of the non-ideality in mixing. The excess volumes at 308.15 and 313.15 K are plotted in Fig. 6a and b, respectively. The greatest deviation from ideality occurred in CO_2-rich solutions, which approached

TABLE 3

Excess enthalpies of mixing (H_m^E) and solution densities (ρ) for (neopentane + CO_2)

x (Neopentane)	H_m^E (J mol^{-1})	ρ (kg dm^{-3})	x (Neopentane)	H_m^E (J mol^{-1})	ρ (kg dm^{-3})
6.29 MPa 310 K			12.5 MPa 308.15 K		
0.0	0	0.172	0.0	0	0.767
0.50	−2640	0.634	0.150	310	0.744
0.860	−640	0.595	0.50	650	0.657
			0.850	290	0.608

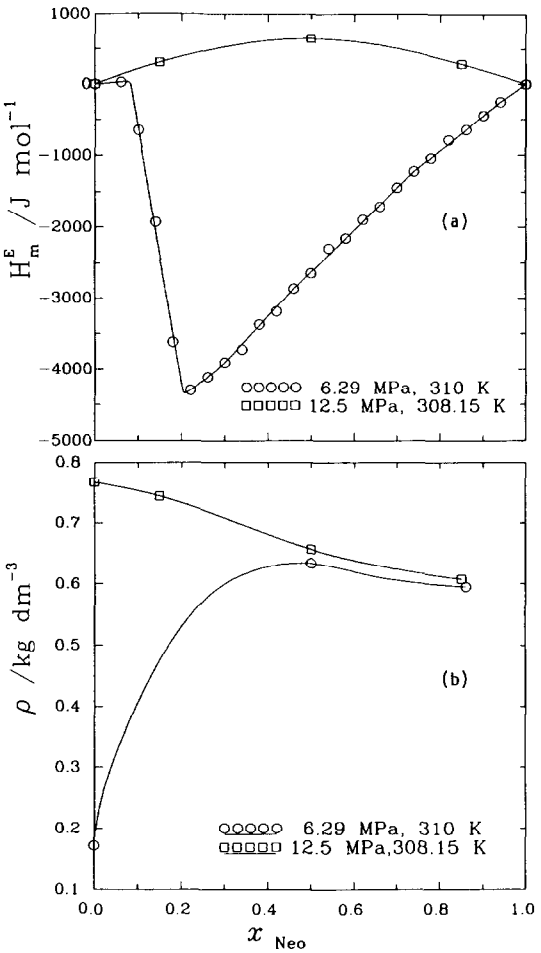

Fig. 7. a, H_m^E (neopentane + CO_2) values as a function of composition [13]; b, densities of (neopentane + CO_2) fluid mixtures as a function of composition.

the critical point more nearly than the hexane-rich solutions. Excess volumes increased as the temperature was raised and the CO_2 volume increased markedly while the liquid volume changed very little.

Neopentane + CO_2

Neopentane was chosen as a component for calorimetry tests with CO_2 because its nearly spherical molecular shape contrasts with that of the linear *n*-hexane and because spherical molecules may be modelled more precisely. Densities and corresponding H_m^E values for selected (neopentane + CO_2) solutions are reported in Table 3. The H_m^E values which were reported earlier [13], are plotted in Fig. 7a. Graphical estimation from Fig. 7a yields the dew point at $x_{neopentane} = 0.08$ and the bubble point at $x_{neopentane} = 0.20$ at 6.29 MPa and 310 K. These values agree well with data reported by Leu and Robinson [14] of 0.063 and 0.213 mole-fraction neopentane at 6.29 MPa and 313.15 K. Densities are plotted in Fig. 7b. At low pressure, the density is seen to rise rapidly from that of the rarefied CO_2 to that of a normal liquid with addition of a small amount of neopentane. The density then decreased with increasing neopentane content of the solutions. At 12.5 MPa, the density decreased steadily as the neopentane content of the solutions increased. Insufficient data were collected to allow computation of V^E and isothermal compressibility values.

SUMMARY

Instrumentation has been developed to measure simultaneously the H_m^E and density values of fluids at specific temperature–pressure coordinates using a flow calorimeter. The instrument has been used to collect H_m^E and density data for (*n*-hexane + CO_2) and (neopentane + CO_2) near the CO_2 critical point. Phase boundaries and isothermal compressibilities were determined from the primary data. Thus, all the information needed to model critical fluid behavior is measured simultaneously. VLE and isothermal compressibility values were derived from the H_m^E and density data. Good agreement with literature data was observed. This instrumentation is proving very useful in collecting the data necessary for developing improved models of fluid properties in the critical region.

ACKNOWLEDGEMENTS

We thank the Bureau of Mines Salt Lake City Research Center for use of the high-pressure densitometer cell. The assistance of Paul Harding and Peter Slater in operating the calorimeter is also appreciated. Financial

support for the research was provided by the National Science Foundation through Grant CHE-8712799.

REFERENCES

1 F.P. Schmitz and E. Klesper, J. Supercritical Fluids, 3 (1990) 29.
2 A.Z. Panagiotopoulos and R.C. Reid, Am. Chem. Soc. Fuel Chem. Div. Preprints, 30 (1985) 46.
3 M.E. Paulaitis, V.J. Krukonis, R.T. Kurnik and R.C. Reid, Rev. Chem. Eng., 1 (1983) 179.
4 J.J. Christensen, L.D. Hansen, D.J. Eatough, R.M. Izatt and R.M. Hart, Rev. Sci. Instrum., 47 (1976) 730.
5 J.J. Christensen, L.D. Hansen, R.M. Izatt, D.J. Eatough and R.M. Hart, Rev. Sci. Instrum., 52 (1981) 1226.
6 G. Morrison, J.M.H. Levelt Sengers, R.F. Chang and J.J. Christensen, Thermodynamic Anomalies in Supercritical Fluid Mixtures, in J.L.M. Penninger, M. Randosz, M.A. McHugh and V.J. Krukonis (Eds.), Supercritical Fluid Technology, Elsevier, Amsterdam, 1985.
7 P.A. Wells, R.P. Chaplin and N.R. Foster, J. Supercritical fluids, 3 (1990) 8.
8 IUPAC, Carbon Dioxide, IUPAC Thermodynamic Tables of the Fluid State, S. Angus, B. Armstrong and K.M. deReuck (Eds.), Pergamon Press, Oxford, 1976.
9 M. Diaz Pena and G. Tardajos. J. Chem. Thermodyn., 10 (1978) 19.
10 J.J. Christensen, T.A.C. Walker, R.S. Schofield, P.W. Faux, P.R. Harding and R.M. Izatt, J. Chem. Thermodyn., 16 (1984) 445.
11 G.M. Schneider, in G.M. Schneider, E. Stahl and G. Wilke (Eds.), Extraction with Supercritical Gases, Verlag Chemie, Deerfield Beach, FL, 1980, pp. 45–81.
12 J.J. Christensen, S.P. Christensen, R.S. Schofield, P.W. Faux, P.R. Harding and R.M. Izatt, Thermochim. Acta, 67 (1983) 315.
13 R.L. Rowley, J.L. Oscarson, R.M. Izatt, W.K. Tolley, P.N. Slater and N.F. Giles, Fluid Phase Equil., 53 (1989) 167.
14 A. Leu and D.B. Robinson, J. Chem. Eng. Data, 33 (1988) 313.